

In search of universal EoS for cold dense matter

Sk Md Adil Imam^{1,2*} and B. K. Agrawal^{1,2}

¹*Saha Institute of Nuclear Physics, 1/AF Bidhannagar, Kolkata 700064, India. and*

²*Homi Bhabha National Institute, Anushakti Nagar, Mumbai 400094, India.*

Our understanding of the equation of state for densely packed matter remains limited, primarily owing to the uncertainties surrounding the symmetry energy at high densities. The nuclear symmetry energy represents a crucial element of nuclear binding energy, and its responsiveness to isospin asymmetry plays a pivotal role in understanding various phenomena within nuclear physics and astrophysics. This concept carries significant implications for our comprehension of nuclear structure, heavy-ion collisions, and the behavior of neutron-rich matter in extreme astrophysical environments like neutron stars and supernovae. However, our understanding of the symmetry energy at densities beyond saturation remains limited. To address this, we leveraged observational data from neutron stars collected by NICER and LIGO to confine our understanding of the high-density symmetry energy. Our constrained equations of state align with terrestrial experiments, ab-initio theoretical calculations, and high-density perturbative QCD constraints.

Introduction

Exploring the QCD phase diagram holds significant importance in the multi-messenger era. While QCD calculations demonstrate reliability at extremely high densities, approximately around 40 times the nuclear saturation density (ρ_0), it is possible to employ an effective theory of QCD that preserves QCD symmetries up to a breakdown scale, which is in proximity to twice the nuclear saturation density. In the intermediate density range, numerous parameterized forms of the equation of state (EoS) exist, but they must align with the observables accessible within that density regime.

The EoS of NS matter we are using can be decomposed in terms of two components as follows

$$\varepsilon(\rho, \delta) = \varepsilon(\rho, 0) + J(\rho)\delta^2 + \dots, \quad (1)$$

where, $\varepsilon(\rho, 0)$ and $J(\rho)$ are the EoS for symmetric nuclear matter and symmetry energy, respectively and $\delta = \left(\frac{\rho_n - \rho_p}{\rho}\right)$ is the isospin asymmetry parameter with ρ_n and ρ_p being the neutron and proton densities, respectively. $\varepsilon(\rho, 0)$ and $J(\rho)$ can be further expanded in terms of various nuclear matter parameters (NMPs) which are e_0 (binding energy), K_0 (incompressibility), Q_0 (skewness), Z_0 (kurtosis) and J_0 (symmetry energy at saturation), L_0 (slope of symmetry energy) $K_{sym,0}$ (curvature), $Q_{sym,0}$, $Z_{sym,0}$, respectively.

We have used astrophysical data from the event GW170817[3] from the LIGO observation and the observational data from the X-ray pulse profile modeling of NS by the NICER [4–7] group and check the consistency of our results with the available data from Heavy Ion Collision (HIC)[9–11] from Symmetric Nuclear Matter (SNM) and symmetry energy and also with the data at low density from N³LO χ EFT[8] and with the data at high density from pQCD[12].

To construct the EoSs we use the $\frac{n}{3}$ (see for details [1]) model for a suitable set NMPs (see Table I) which satisfies the condition of i) Thermodynamic stability ii) $J(\rho) \geq 0$ iii) Causality iv) The EoS should give maximum mass of stable neutron star greater than $2.15 M_\odot$.

TABLE I: Priors for the NMPs used in our analysis. All the parameters are uniformly distributed within the minimum ('min') and maximum ('max') bounds. The median ('med') values are also listed [2]. All values are in the units of MeV.

NMP	min	max	med
e_0	-16.3	-15.7	-16.0
K_0	200	300	231.96
Q_0	-800	-800	-418.89
Z_0	1400	2500	1638.14
J_0	27	37	31.87
L_0	20	120	52.26
$K_{sym,0}$	-250	250	-67.44
$Q_{sym,0}$	300	900	726.29
$Z_{sym,0}$	-2000	-1000	-1622.35

Results and Discussions

We have constructed an extensive set of equation of state (EoS) variations based on the distribution of nuclear matter parameters (NMPs) as listed in Table 1, ensuring their compatibility with the specified condition discussed above. The EoSs have been constrained using astrophysical data, with a particular focus on the symmetry energy:

i) Tidal deformability constraint from GW170817

ii) Mass-Radius posterior from NICER.

In Figure 1, we present the mass-radius distribution at various stages of constraint application. Figure 1(a) represents the initial state or 'prior' distribution. After implementing the $1.4 M_\odot$ constraint, it is evident from Figure 1(b) that a significant number of EoSs have been excluded. Similarly, Figure 1(c) illustrates that applying the $2.08 M_\odot$ constraint further narrows down the permissible EoSs. However, when both constraints (i) and (ii) are combined, the number of allowable EoSs is significantly reduced, shown in Fig 1(d). This observation underscores the potential for future precise measurements and measurements at different masses to further constrain the equation of state.

In Figure 2, we illustrate the distribution of the EoS under different applied constraints. In Figure 2(a), we depict the pressure as a function of energy density at

*Electronic address: skmdadilimam@gmail.com

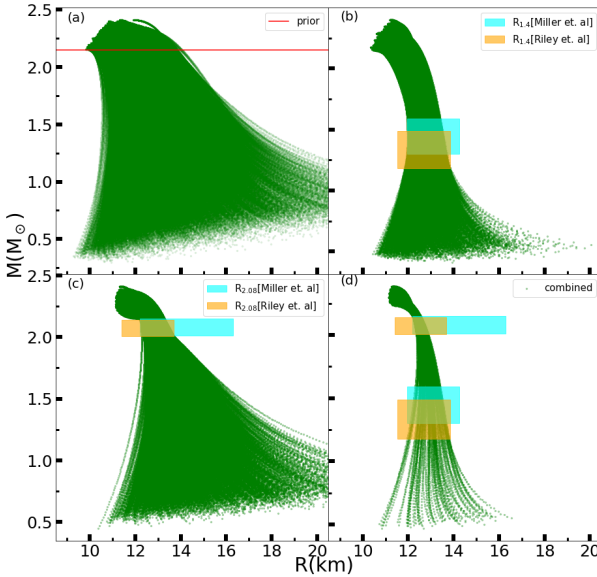


FIG. 1: (color online)Neutron Star Mass-Radius Distributions: (a) Represents the initial or prior distribution, (b) Illustrates the cumulative impact of the prior and $1.4 M_{\odot}$ constraints, (c) Demonstrates the combined effect of the prior and $2.08 M_{\odot}$ constraints, and (d) Depicts the outcome of incorporating all utilized astrophysical data.

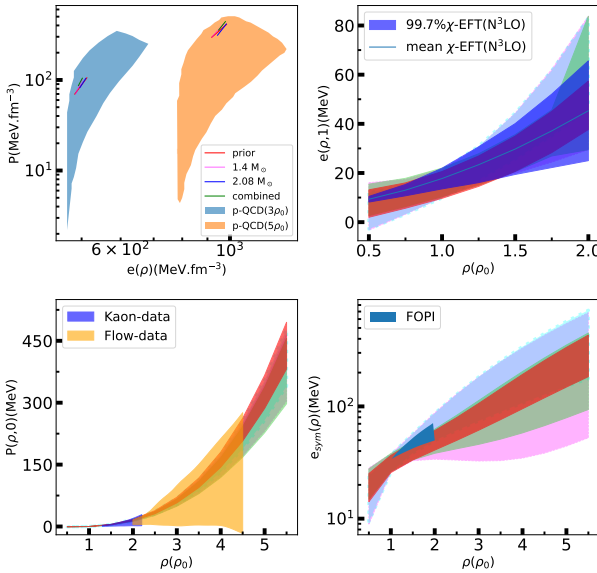


FIG. 2: Distribution of Equation of States (EoSs): Figure (a) illustrates the distribution of pressure and energy density at various constraint application stages. Figure (b) presents the energy distribution for pure neutron matter, $e(\rho, 1)$, while (c) showcases the pressure distribution for symmetric nuclear matter, $P(\rho, 0)$. Lastly, (d) displays the outcomes for symmetry energy, $e_{sym}(\rho)$. All results are presented at a 95% confidence interval.

baryon densities of $3\rho_0$ and $5\rho_0$. Our EoSs, which are exclusively constrained by astrophysical data, exhibit consistency with the region allowed by perturbative QCD(pQCD). Notably, the application of the $1.4 M_{\odot}$ constraint tends to favor a softer EoS, while the

$2.08 M_{\odot}$ constraint inclines towards a stiffer EoS.

Figure 2(b) displays the energy of pure neutron matter (PNM). The combined constraints align well with the low-density PNM constraints derived from Chiral Effective Field Theory (χ EFT).

In Figure 2(c), we display the pressure for symmetric nuclear matter $P(\rho, 0)$. Once again, it becomes apparent that the combined constraints push for a stiffer EoS. We have also included data from Heavy Ion Collisions (HIC) for comparison, and our final posterior of the symmetric nuclear matter pressure is consistent with the considered HIC data.

Lastly, in Figure 2(d), we depict the symmetry energy, denoted as $e_{sym}(\rho)$, as a function of baryon density. The combined constraints, represented by the red band, significantly reduce the uncertainty at high densities. For context, we have included data for $e_{sym}(\rho)$ from the FOPI group's Heavy Ion Collisions (HIC) as well.

The nuclear matter parameters which are well constraint for the combined constraint are slope and the curvature of symmetry energy L_0 and K_{sym0} respectively. The combined constraints necessitate that both the slope and curvature exhibit reduced values compared to high mass constraints used.

We have developed our equation of state (EoS) by amalgamating a subset, $\frac{n}{3}$, of EoSs that adhere to stability, causality, non-negativity of the symmetry energy, and have the capability to produce neutron stars with a minimum mass of $2.15 M_{\odot}$. Within this selection, we have identified a collection of EoSs that, when constrained solely by astrophysical data, exhibit alignment with terrestrial data, ab initio nuclear physics constraints at low densities, as well as perturbative Quantum Chromodynamics constraints at high densities.

References

- [1] Imam et al., Phys. Rev. C, **105**, 015806 (2022).
- [2] Patra et al., Phys. Rev. D, **106**, 043024 (2022).
- [3] Abbott, B. P. et al., Phys. Rev. Lett., **119**, 161101 (2017) L27 (2021).
- [4] Miller, M. C. et al., Astrophys. J. Lett., **887**, L24 (2019).
- [5] Riley, T. E. et al., Astrophys. J. Lett., **887**, L21 (2019).
- [6] Miller, M. C. et al., Astrophys. J. Lett., **918** L28 (2021).
- [7] Riley, T. E. et al., Astrophys. J. Lett., **918** L27 (2021).
- [8] J. Lattimer, Annual Review of Nuclear and Particle Science **71**, 433 (2021).
- [9] Lynch, W G et al., Prog. Part. Nucl. Phys. **62**, 427 (2009).
- [10] Danielewicz, P et al., Science **298**, 1592 (2002)
- [11] A. Le F'evre et al., C. Hartnack, Nucl. Phys. A **945**, 112 (2016)
- [12] Komoltsev, Oleg and Kurkela, Aleksi, Phys. Rev. Lett. **128**, 202701 (2022)